



Groundwater Quality Assessment and Geochemistry in the Guerrara Region, Algeria

Benameur Farid¹, Slimani Rabia², Hamdi Aissa Baelhadj³

¹Laboratory of Research on Phoeniculture "Phoenix", Faculty of natural and life sciences, University of Kasdi Merbah, Ouargla, Algeria, Email: benameur.farid@univ-ouargla.dz, <https://orcid.org/0000-0002-7129-3918>

²Laboratory of Biogeochemistry of Desert Environments. Department of Agronomic Sciences, University of Kasdi Merbah, Ouargla, Algeria, E-mail: slm_rabia@yahoo.fr

³Laboratory of Biogeochemistry of Desert Environments. Department of Agronomic Sciences, University of Kasdi Merbah, Ouargla, Algeria E-mail: hamdi_30@yahoo.fr

Submission : 11/06/2025.

Acceptation: 23/05/2026

Abstract

The investigation in question involved the collection of 85 groundwater specimens from Complex Terminal aquifer wells in the Guerrara region. The purpose was to appraise the chemical quality of the water and examine the hydrochemical operations that influence the mineral content of the groundwater. The data obtained revealed that the water samples showcased a slightly alkaline pH and had high mineral concentrations. The order of decreasing concentration of the mainstream ions present in the water is as follows: sulfate ion (SO₄²⁻), chloride ion (Cl⁻), sodium ion (Na⁺), calcium ion (Ca²⁺), bicarbonate ion (HCO₃⁻), magnesium ion (Mg²⁺), nitrate ion (NO₃⁻), and potassium ion (K⁺). The Geographic Information System (GIS) was utilized to visually represent the spread of parameters across the area under study. Hierarchical Component Analysis (HCA) was employed to identify four distinct geochemical water facies: SO₄-Na-Ca, SO₄-Na-Cl, SO₄ with no dominant cation, and SO₄-Cl-Na-Ca. Principal Component Analysis (PCA) was implemented to categorize water parameters into three principal components (PCs) that represented 72.66% of the overall variance. The analysis revealed that the foremost sources of water mineralization are the dissolution of evaporitic and carbonate rocks, as well as anthropogenic activities. The Saturation Index indicated that the water samples were supersaturated with respect to calcite and dolomite, while being undersaturated with regard to gypsum, anhydrite, and aragonite. Geochemical plots demonstrated that evaporation and the interaction between rocks and water, particularly through the base ion exchange process, are the key mechanisms influencing groundwater mineralization.

Keywords: Water, GIS, PCA, Chemical quality, Guerrara

Introduction

There has been a growing interest in studying groundwater aquifers in arid regions with limited and unpredictable rainfall in recent years. These aquifers are crucial for meeting human needs such as drinking water, agricultural development, and industrial activities (Nadhira and Omar 2019; Slimani et al. 2023). The North-Western Sahara Aquifer System (NWSAS) (Brauch et al. 2011), spans Algeria, covering 700,000 km²; Libya, covering 250,000 km²; and Tunisia, covering 80,000 km² in North Africa (Dhaoui et al. 2016; Benaraba et al. 2022). The aquifer system in question covers an area of around one million km² and is recognized as the second-largest aquifer system globally, surpassed only by the Nubian Sandstone (Dhaoui et al. 2016). It is the primary water source for the Sahara Desert (Li et al. 2024) and consists of three major Saharan aquifers, namely the Continental Intercalaire, the Complexe Terminal and the phreatic aquifer (OSS 2003; Slimani et al. 2017; Guendouz and Moulla 2010; Castany 1982). The Complex Terminal aquifer extends across the majority of the Algerian and Tunisian sedimentary basins, including an area exceeding 350,000 km² and it is predominantly unconfined (Guendouz et al. 2003). This aquifer exhibits a notable increase in the number of boreholes (over 5,300 boreholes), resulting in the extraction volume from the aquifer surpassing the volume replenished by recharge. Other hazards to the aquifer encompass water salinization, the depletion of artesian wells, the drying up of outlets, and excessive pumping elevations (Swezey 1999). Agriculture is the primary occupation in the Guerrara oasis (Lower-Sahara, Algerian), and it heavily relies on groundwater for irrigation. The irrigation water is supplied from three main reservoirs: the unconfined alluvial aquifer, the Continental Intercalary aquifer, and the Complex Terminal aquifer. In recent times, the alluvial water has experienced a decline in quality, transitioning from being low in salt content to becoming overly salty. This change has harmed the soil quality and agricultural productivity (Khemgani et al. 2019). In addition, the scarcity of Continental Intercalary deep wells has compelled farmers to resort to constructing Complex Terminal wells, which are relatively shallow and inexpensive, in order to ensure an adequate water supply for irrigation and to expand their agricultural operations. The hydrochemical quality of the water from Algeria's Complex Terminal aquifer has been the subject of numerous studies (Reghais et al., 2023; Barkat et al., 2021; Kherroubi et al., 2022). However, this study uniquely assesses the appropriateness of Complex Terminal water for consumption and irrigation, while analyzing the hydrochemical conditions and underlying processes in the reservoir aquifer of the Guerrara region. The main objectives of this study are to (1) assess the physicochemical

properties of Complex Terminal water, (2) create a GIS-based map of chemical parameters, (3) determine the water quality of the Complex Terminal water, through WQI analysis (4) discuss the suitability of the water for drinking, agricultural and industrial purposes.

Hydrochemical evaluation is conducted using several tools such as Statistical Analysis, Saturation Index, Gibbs diagram, Chadha plot, and Ionic Plots. The water quality index (WQI) is employed to verify the potability of water. Sodium Adsorption Ratio (SAR), Electrical Conductivity (EC) (Madjeed et al. 2021), Residual Sodium Bicarbonate (RSBC), SSP (Soluble Sodium Percentage), Magnesium Percentage (Mg%), Kelly's Ratio (KR), Potential Salinity (PS), Permeability Index (PI), and the Chloralkaline Index (CAI) are employed to assess the suitability of water for irrigation purposes (Sangaré et al. 2023). This study should be a useful resource for the scientific community and for decision makers involved in the sustainable management of groundwater.

Materials and Protocols

Investigation area display

The research area is 600 kilometers south of Algiers in the Ghardaia province in the northern Algerian desert. The location is approximately 2,900 Km², with geographical coordinates of 32° 47'25"N latitude and 4° 29'32"E longitude. The population exceeds 70,000. Guerrara is renowned for being a highly productive agricultural area specializing in growing palm trees, olives, and citrus fruits. It also supports livestock farming, particularly cattle and sheep. The National Meteorological Office (2023) states that the area experiences hyper-arid climatic conditions, with hot summers and mild winters. The annual precipitation is meager, with an average of 81 mm. The average minimum temperature fluctuates between 3 and 17 degrees, with an average of 10 degrees, and the average maximum temperature fluctuates between 28 to 40 degrees, with an average of 34 degrees.

Geology and hydrogeology

The study area has three types of geological formations: the upper cretaceous, which extends from west to east and to the Northwestern part of Guerrara (fig. 1); the Neogene or Mio-pliocene; and the Continental Pliocene, which is an extended form of thick and continuous limestone; and the Continental Quaternary, which is presented as river alluvium by the Saharan sedimentary formations (S.C.G 1952; Hadj-said et al. 2013; Chellat et al. 2014). The Middle Pliocene formation is prominent in the central and southeastern areas, characterized by sand, clay, argillaceous sand, and gypsum crystals. In the eastern region, the Middle Pliocene deposit transitions to the Eocene epoch, with a decrease in rock thickness and composition of carbonate Eocene and evaporative Eocene, comprising limestone and marl limestone (Chellat et al. 2014). The Wadi Zegrir River exhibits sedimentary layers including alluvium, rocky desert areas, and sand dunes, indicating the Quaternary period (Djili and Hamdi-Aïssa 2018).

The aquifers exhibiting the hydrogeological traits of the region are the following: firstly, the alluvial aquifer located at the surface, with a depth ranging from 3 to 30 meters, according to Melouah & Zeddouri (2016), the Complex Terminal aquifer includes mainly the Mio-Pliocene, Eocene, and Senonian aquifers, the Senonian aquifer covers a thickness of approximately 275 meters, while the Mio-Pliocene and Eocene aquifers are approximately 200 meters thick. At the bottom, there is the Intercalary Continental aquifer, which has an average thickness of 650 meters. The intermittent water flow in Wadi Zegrir reflects the hydrological features of the research area (Melouah et al. 2020). Figure 1 depicts the cross-section representing the hydrogeological structures of the study area created using the Strater 5 program. The cross-section is based on five end-of-borehole reports that focus on the intercalary continental aquifer at various locations within the Guerrara region.

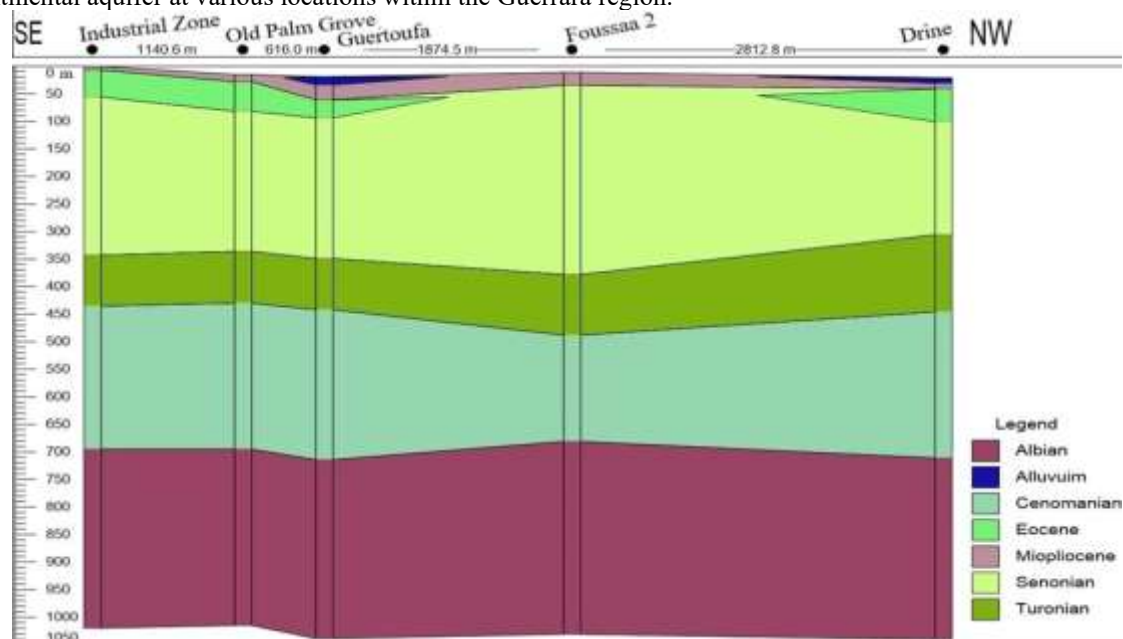


Fig.1 Hydrogeological cross-section of the research area.

Methods for sampling and analysis

Eighty-five samples were obtained from wells located in agricultural farms around four sampling campaigns between 2020 and 2022. The sampling of wells over the research region needs to be more balanced. To do this, we gathered samples from most agricultural boundaries. Figure 2 displays the spatial arrangement of wells in the research region using a Digital Elevation Model (DEM) acquired from the United States Geological Survey website (US Geological Survey, 2023). The model has a precision of 12.5 meters and the study area's boundaries were established using contour topography. The sampling, storage, and analysis procedures were conducted per international standards. The physicochemical parameters, which are temperature, pH, and electrical conductivity (EC), were documented on-site utilizing a Multiparameter portable meter (Multiline ® Multi 3630 IDS). Before taking samples, the polyethylene bottles underwent a preliminary cleaning process consisting of one wash with deionized water and three washes with sample water. After a short period of extracting water from wells, samples are collected and subsequently kept at 4°C until they can be analyzed in the laboratory (Khan et al. 2020). The primary chemical constituents (Ca^{2+} , K^+ , Na^+ , Mg^{2+} , HCO_3^- , Cl^- , SO_4^{2-} , and NO_3^-) were analyzed at the biogeochemistry laboratory of desert environments at the University of Ouargla. The contents of sodium and potassium were estimated with a flame photometer (PFP7 Jenway), while sulfate and nitrate concentrations were determined using a DR2000-HACH spectrophotometer (Bouselsaland Saibi. 2022). To measure calcium and magnesium content, complexometric titration is used in the presence of an Ethylene Diamine Tetra Acetic (EDTA) solution. The volumetric titration procedure employing 0.1 N hydrochloric acid is used to determine the bicarbonate concentration (Nayak et al. 2022). Chemical tests of water samples are considered valid only if the ionic balance is equal to or less than 5% (Rodier. 1996).

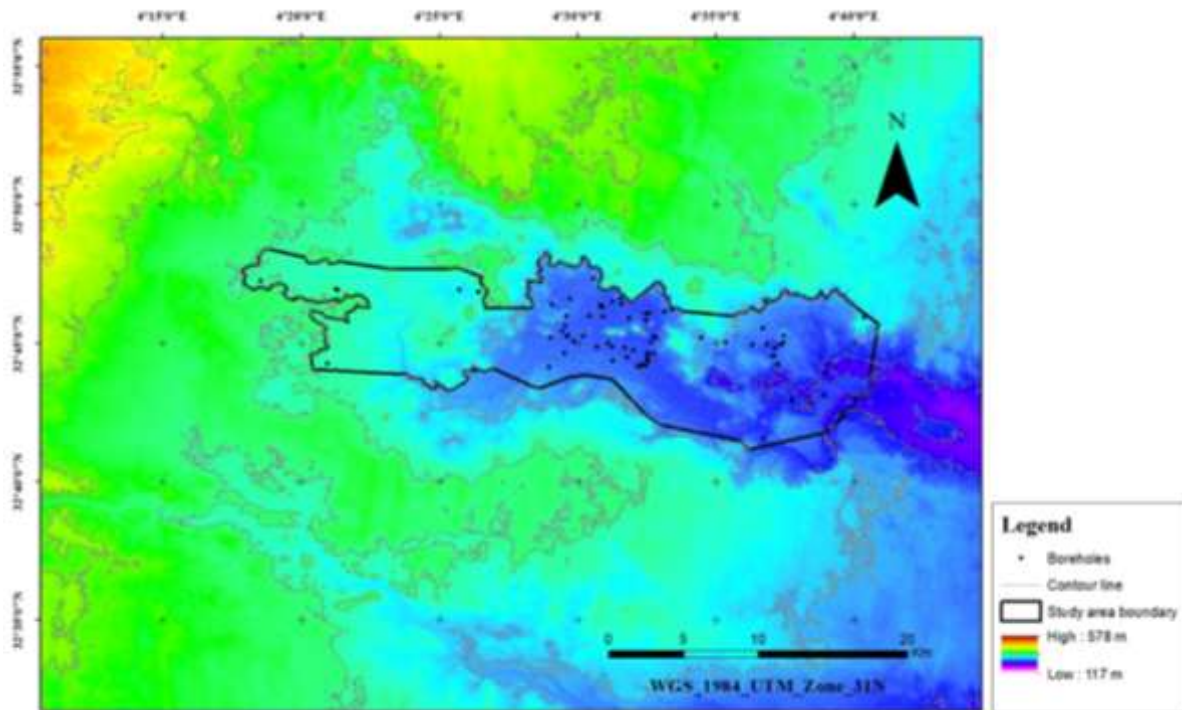


Fig. 2 Geographical dispersion of wells across the research area on a Digital Elevation Model (DEM) with a precision of 12.5 meters.

All the results are displayed in mg/l except EC which is expressed in IS/cm. For better accuracy of the water quality results, the ionic balance was calculated for selected cations (Ca, Mg, Na, K) and anions (HCO_3 , Cl, SO_4 , NO_3), and the error was in between $\pm 10\%$ and which is well within the limit. The application of factor analysis to the whole dataset to simplify the large dataset with proper arrangement, and by generalizing, it leads to meaningful interpretation. Statistical package for social sciences (SPSS) is used for statistical analysis and to draw the relations. As per the standard statistical procedures, the data have been standardized. The factor analysis and factors extraction were done with the PCA technique.

In this research, the methodological for assessing the water quality of the Complex Terminal aquifer in the Guerrara region. This framework integrates statistical methods, GIS techniques, and hydrochemical analysis of water data, as illustrated in Fig. 3.

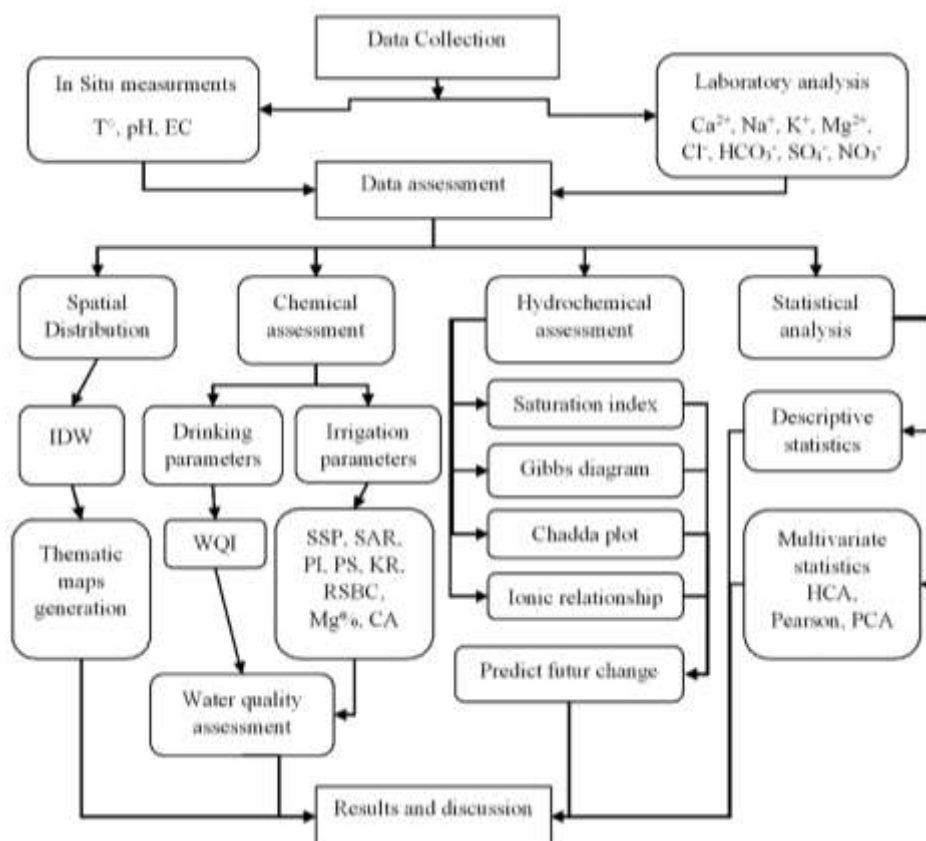


Fig. 3. Flow chart of the methodology used to assess water quality.

Results and discussion

Physicochemical characteristics

Tables 1 and Figure 4 present the results of the physicochemical analyses. The pH ranges from 7 to 7.93, with a typical value of 7.40, signifying neutral to slightly alkaline circumstances. The electrical conductivity (EC) at 25°C varies from 701 to 7298 $\mu\text{S}/\text{cm}$, with an average of 2903.16 $\mu\text{S}/\text{cm}$. Total dissolved solids (TDS) have an average of 1993.03 mg/l and range from 419 to 5084 mg/l. Sodium is the most concentrated cation, with values between 57.18 and 1103.48 mg/l, and a mean of 329.11 mg/l. Next comes calcium, which has an average of 207.22 mg/l and a range of 38.71 to 508.35 mg/l. The range of magnesium values is 1.74 to 270 mg/l, with an average of 79.93 mg/l. Potassium concentrations vary from 1.32 to 34.4 mg/l, with a mean of 9.31 mg/l. The dominant anion is sulfate, ranging from 152.7 to 1924 mg/l, and averaging 737.76 mg/l. Chloride concentrations vary between 73.5 and 1858.3 mg/l, with a mean of 462.81 mg/l. The concentration of bicarbonate ranges from 19.8 mg/l to 378.2 mg/l, with an average of 156.1 mg/l. Nitrate concentration vary from 0 mg/l to 37mg/l, with an average of 10.7mg/l.

Table 1 Statistical propertises of the analysed data

Statistical properties	pH	TDS	EC	Na ⁺	K ⁺	Ca ²⁺	Mg ²⁺	Cl ⁻	SO ₄ ²⁻	HCO ₃ ⁻	NO ₃ ⁻
Median	7.40	1778	2578	280	5.62	174.40	68.64	317.15	663.80	146.40	7.80
Skewness	0.14	1.17	1.13	1.58	1.42	1.37	1.11	1.41	1.09	1.20	1.23
Coef. of variation (%)	3.2	53	50.8	69.9	82.5	60.6	67.3	75.6	54.2	33.9	77.3
Confidence interval 95% Lower Bound	7.35	1756.35	2585.17	279.52	7.65	180.13	68.34	387.37	651.47	144.69	8.92
Confidence interval 95% Upper Bound	7.45	2220.71	3221.16	378.70	10.96	234.31	91.53	538.24	824.05	167.52	12.49
Dist. characteristics (Kolmogorov-smirlov signification)	0.929	0.077	0.085	0.005	0.000	0.013	0.138	0.007	0.093	0.308	0.001

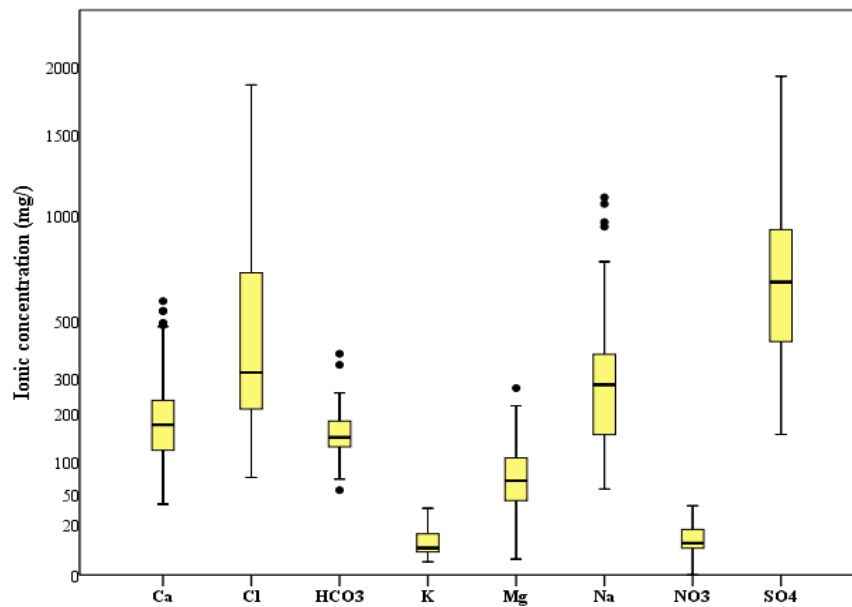
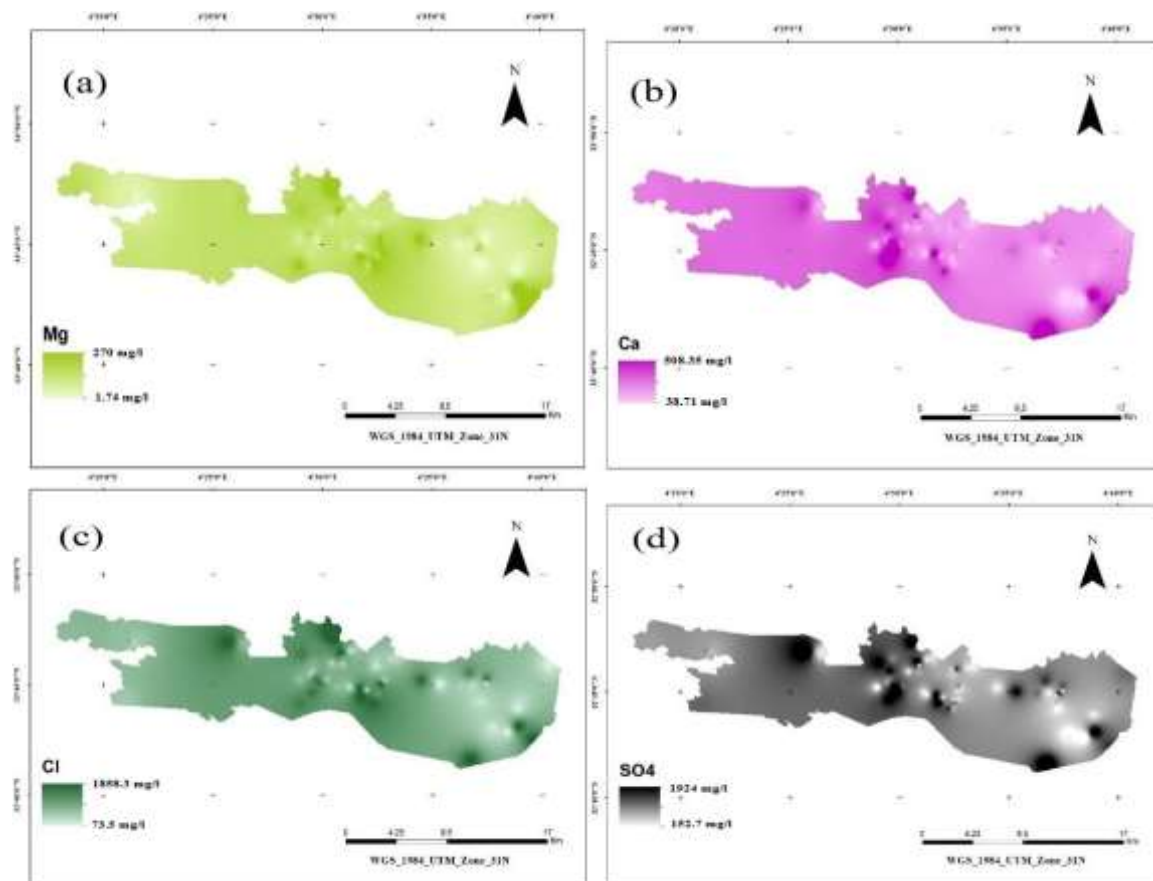


Fig.4. Box plots showing the concentration of water parameters with outlier data

The geographical dispersion of mineralization

The regional distribution of sulfates, chlorides, and sodium within the scope of the study region positively correlates with the geographical dispersion of Electrical Conductivity, suggesting that those charged particles are the primary contributors to water mineralization (Fig. 5; 6). The center and eastern regions of the examined area, close to the old palm grove of Guerrara Oasis and the new agricultural perimeters, exhibit the highest levels of electrical conductivity, sulfates, chlorides, and sodium. Groundwater over pumping at the Complex Terminal causes an accumulation of salts in the water due to the dissolving of the underlying rocks of the aquifer, which primarily consist of gypsum, anhydrite, halite, calcite, and dolomite.



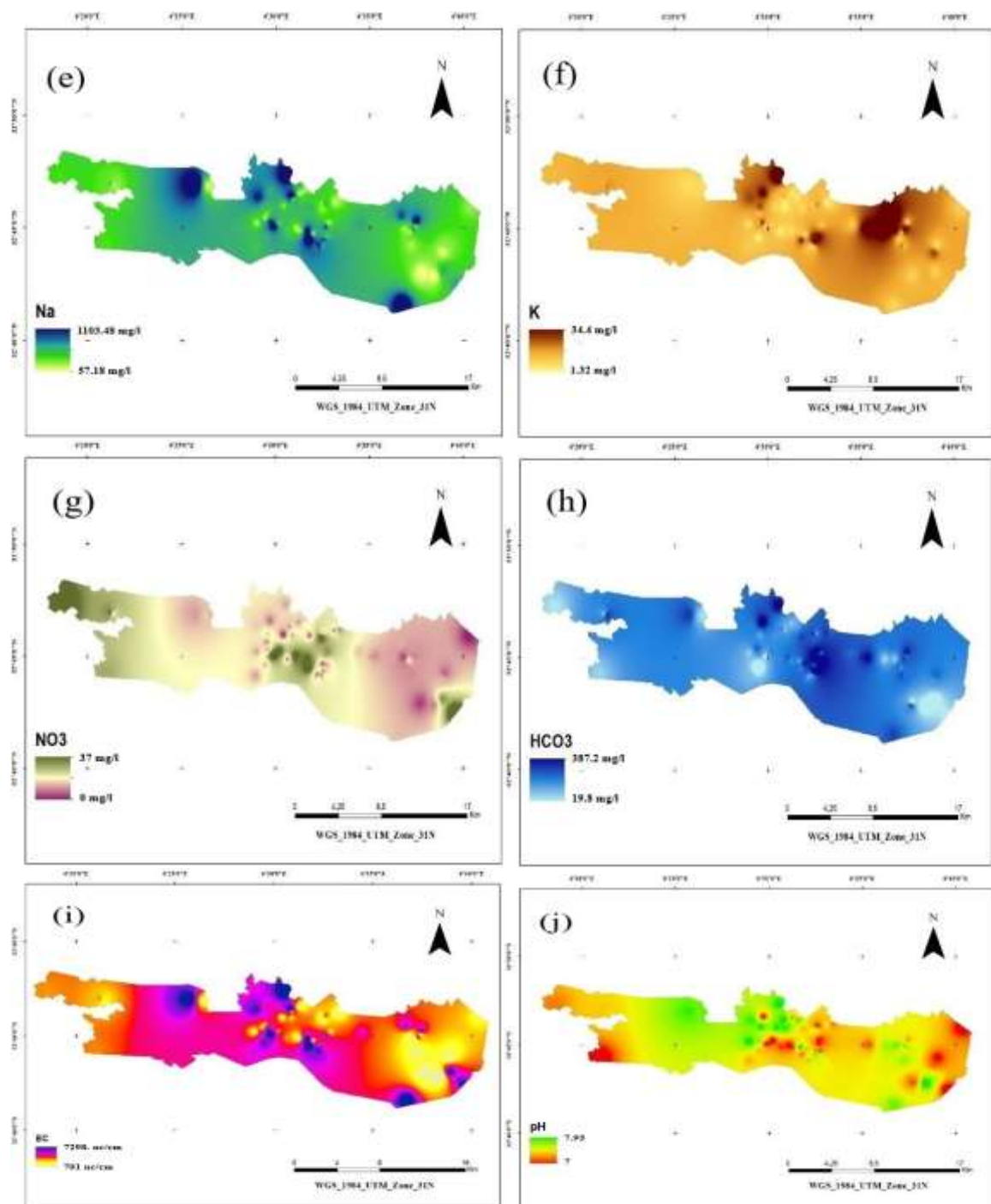


Fig. 5. Geographical dispersion map of (a) Mg, (b) Ca, (c) Cl, (d) SO₄, (e) Na, (f) K, (g) NO₃, (h) HCO₃, (i) EC and (j) pH values using Inverse Distance weightings as a method of interpolation.

Hierarchical component analysis and hydrochemical facies

Hierarchical component analysis (HCA) is a data analysis method that categorizes groundwater wells into four distinct groups based on their similar chemical makeup. The groups from 1 to 4 are visually represented in the dendrogram shown in Figure 8 and table 2.

- Group 1 consists of 30 wells. The average electrical conductivity is 1957.03 $\mu\text{s}/\text{cm}$, with a range of 701 to 4707 $\mu\text{s}/\text{cm}$. According to the Piper diagram, the hydrochemical facies SO₄-Ca-Na distinguish this group.
- Group 2 consists of 12 wells; the average electrical conductivity is 3594.41 $\mu\text{s}/\text{cm}$, ranging from 1970 to 7298 $\mu\text{s}/\text{cm}$; the hydrochemical facies SO₄-Cl-Na differentiate this group according to the Piper diagram (Fig. 7).
- Group 3 comprises 23 wells. The electrical conductivity goes from 1383 and 4267 $\mu\text{s}/\text{cm}$, the average is 2369.26 $\mu\text{s}/\text{cm}$. Depending on the Piper diagram analysis, sulfate (SO₄²⁻) and chloride (Cl⁻) anions with no prevailing cation are the dominant facies of this group.
- Group 4, which consists of 20 wells, has an average electrical conductivity of 4521.6 $\mu\text{s}/\text{cm}$ and a range of 2337 to 7119 $\mu\text{s}/\text{cm}$. The Piper diagram indicates that the hydrochemical facies of SO₄-Cl-Ca-Na distinguish this group.

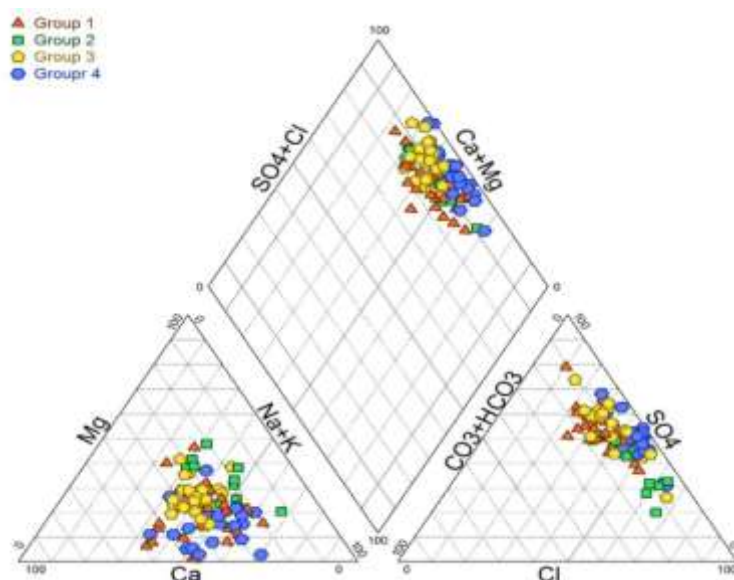


Fig.7. Piper diagram.

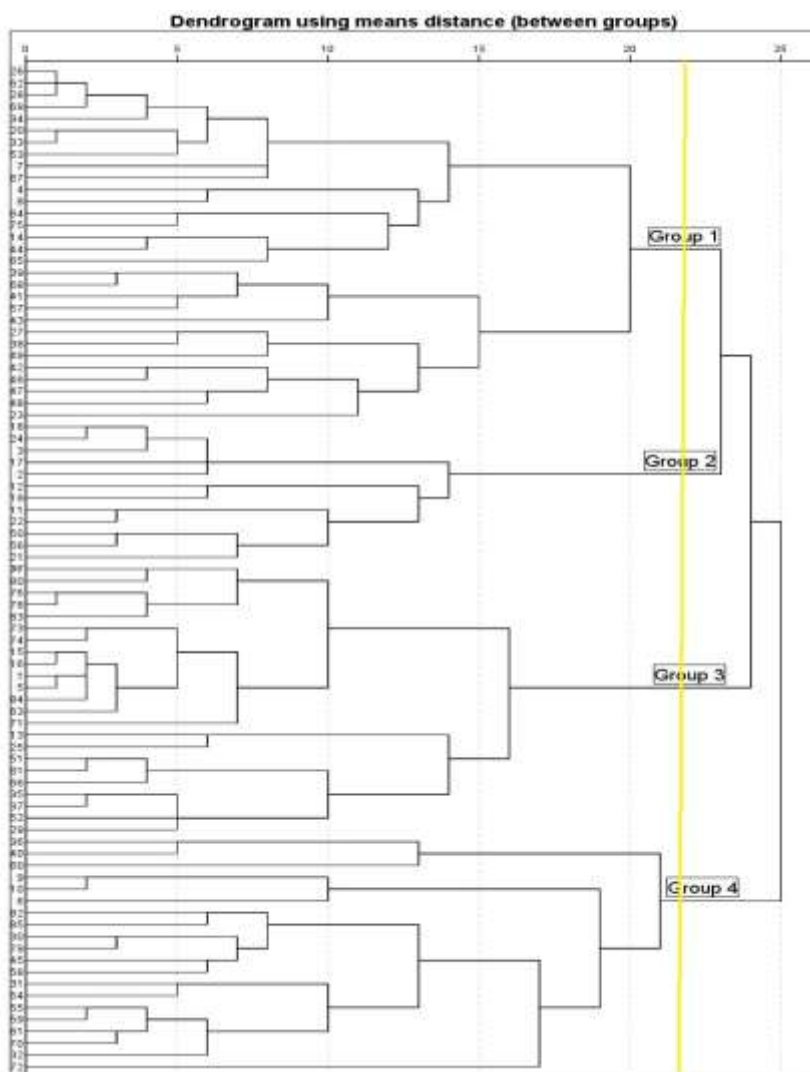


Fig.8. Dendrogram for groundwater samples.

Table 2 Descriptive statistics for water groups (SD: Standard Deviation)

Chemical parameter	T (°C)	pH	EC (µs /cm)	Ca ²⁺ (mg /l)	Na ⁺ (mg /l)	K ⁺ (mg / l)	Mg ²⁺ (mg / l)	Cl ⁻ (mg / l)	SO ₄ ²⁻ (mg / l)	HCO ₃ ⁻ (mg / l)	NO ₃ ⁻ (mg / l)
Min	20.8	7.2	701	38.71	57.18	1.32	1.94	73.5	152.7	55.6	0.05

	Max	26.1	7.93	4707	286.4	625.27	34.4	124	855	1225	201.3	22.1
	Mean	24.03	7.52	1957.03	140.79	213.04	10.4	46.17	240	525.73	147.06	7.33
	SD	1.2	0.17	831.37	61.48	128.34	8.54	30.93	152	276.53	40.46	4.21
Group 2	Min	21.2	7	1970	115.06	148.9	2.1	83.12	251.1	414.78	131.8	0
	Max	25.6	7.75	7298	382.87	939.03	32.5	270	1858	1299.9	378.2	17.69
	Mean	23.62	7.3	3594.41	175.36	401.43	16.4	143.78	706.5	727.52	237.5	7.6
	SD	1.11	0.28	1356.5	75.27	225.01	8.96	55.54	416.7	281.77	66.01	6.56
Group 3	Min	23.9	7	1383	53.67	128.79	2.33	33.6	124.3	344.36	104	0.2
	Max	29.9	7.75	4267	378.35	372.93	14	221.61	859.4	1163	195.2	30
	Mean	26.44	7.26	2369.26	180	223.53	5.74	83.23	335.8	628.03	142.66	15.31
	SD	1.65	0.18	770.29	77.31	76.64	2.74	43.7	208.9	223.6	24.41	8.97
Group 4	Min	22.3	7.06	2337	141.53	255.66	1.86	16.04	263.9	535.09	19.8	0.06
	Max	26.3	7.84	7119	580.35	1103.5	23.3	172	1355	1924	198.9	37
	Mean	24.64	7.44	4521.6	357.27	581.24	7.51	88.47	796.9	1188.1	136.3	12.32
	SD	1.13	0.23	1408.68	146.82	259.78	6.45	53.4	318.6	433.45	41.56	10.23

Pearson correlation

Pearson correlation is a statistical approach that determines the level and trajectory of the linear relationship between two variables (Dehbozorgi and Kunuki, 2023). The Pearson correlation coefficient is employed to appraise the associations and disparities among groundwater samples based on physicochemical parameters and the concentration of major ions (El-Rawy et al., 2023). Shoff et al. (2015) state that the correlation coefficient runs from -1 to +1. A correlation is considered high when the coefficient is between ± 0.8 and ± 1.0 , moderate when it is between ± 0.5 and ± 0.8 , and weak when it is between ± 0.0 and ± 0.5 . The strong relationships between electrical conductivity and calcium, sodium, chloride, and sulfate ions provide evidence that these ions are the primary contributors to the mineral content of groundwater. A robust association was also seen between the sodium cation and the chloride and sulfate anions. Calcium cations exhibit a significant association with sulfate. The observed outcomes can be attributed to the interaction between water and the adjacent rocks, which consist of gypsum, anhydrite, calcite, dolomite, and halite, hence influencing the composition of the water.

Table 3 Pearson correlation coefficient values

	T	pH	EC	Na ⁺	K ⁺	Ca ²⁺	Mg ²⁺	Cl ⁻	SO ₄ ²⁻	HCO ₃ ⁻	NO ₃ ⁻
T	1										
pH	-0.271	1									
EC	0.1	0.169	1								
Na ⁺	0.007	0.264	0.951	1							
K ⁺	-0.119	0.069	0.324	0.327	1						
Ca ²⁺	0.247	0.102	0.813	0.711	0.153	1					
Mg ²⁺	0.095	-0.124	0.548	0.363	0.194	0.239	1				
Cl ⁻	0.019	0.175	0.945	0.876	0.29	0.698	0.624	1			
SO ₄ ²⁻	0.219	0.14	0.895	0.858	0.286	0.855	0.352	0.713	1		
HCO ₃ ⁻	-0.143	-0.137	0.166	0.174	0.305	-0.1	0.349	0.18	-0.01	1	
NO ₃ ⁻	0.263	-0.235	0.204	0.145	-0.132	0.259	0.189	0.17	0.207	0.063	1

Principal component analysis (PCA)

Principal component analysis (PCA) is a statistical method used to reduce the number of parameters in a dataset, reducing them to a smaller set to avoid linearity issues (Karamizadeh et al., 2013; Kurita, 2019). It is commonly used to assess and analyze surface and groundwater quality, revealing changes over time and space (Mohammadi 2009). PCA identifies correlations and reduces data into principal components (PCs) that account for a percentage of total variances in chemical parameters (Yang et al. 2021). The variances are linked to the chemical parameters

with the highest loading components, which serve as benchmarks to determine geochemical processes (Liu et al. 2020).

In Table 4, PCA was conducted with an eigenvalue of 1, resulting in the extraction of three compounds. These three principal components (PCs) explained 72.66% of the total variance and are selected to represent the hydrochemical process influencing groundwater mineralization. The first principal component explains 43.85% of the total variation. It is mainly associated with EC, Na⁺, Ca²⁺, Cl⁻, and SO₄²⁻, suggesting that the primary origin of mineralization in the groundwater is the dissolving of evaporitic rocks, specifically NaCl, KCl, CaSO₄, CaSO₄·2H₂O, Na₂SO₄, and CaCl₂. The second principal component accounts for 15.42% of the total variance and is primarily associated with HCO₃⁻, Mg²⁺, and K⁺, suggesting the leaching and dissolution of carbonate minerals such as CaCO₃, MgCO₃, and CaMgCO₃. The third principal component represents 13.39% of the total variance. It is mainly linked to NO₃⁻, pH, and water temperature, indicating pollution sources from human activities such as agricultural fertilizer use, wastewater seepage, and animal waste (Fig. 9).

Table 4 loadings of variables on PCs, eigen values, variability and cumulative percent.

Variable	PC1	PC2	PC3
T°	0.135	-0.194	0.703
EC	0.963	0.244	-
Na	0.927	0.184	-
K	0.273	0.515	-0.308
Ca	0.881	-0.127	0.188
Mg	0.394	0.634	0.273
Cl	0.878	0.317	-
SO ₄	0.928	-	0.110
HCO ₃	-	0.849	-
NO ₃	0.210	-	0.676
pH	0.311	-0.309	0.699
Eigen value	4.823	1.697	1.473
Variability(%)	41.691	15.772	15.205
Cumulative(%)	41.691	57.463	72.668

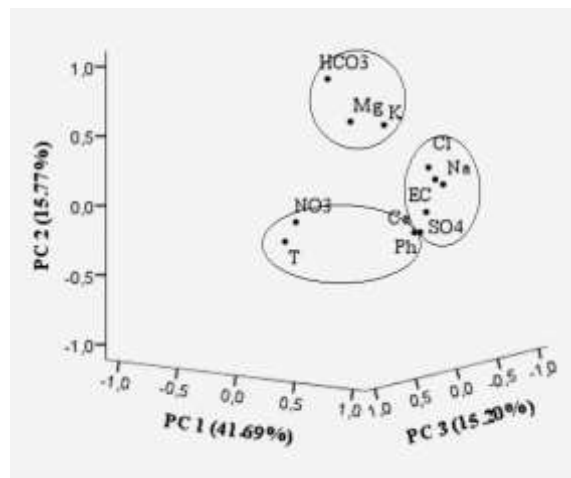


Fig.9. Principal Component Analysis plot

Saturation Index

The saturation index is commonly employed to measure the saturation level (Hwang et al. 2017). The equation $SI = \log(IAP/K_{sp})$ represents the relationship between the saturation index (SI), the ion activity product (IAP) of the mineral groundwater action, and the equilibrium constant (K_{sp}) (Roy et al. 2021). When a mineral and an aqueous solution are in equilibrium, the saturation index (SI) approaches zero. The saturation index (SI) is negative if a solution is sub-saturated while supersaturated solutions have a positive value for the saturation index (SI) (Plummer et al. 1983). The saturation index was determined using PHREEQC version 3, a computer tool for conducting various aqueous geochemical studies (Parkhurst and Appelo 2013). Table 5 displays the findings of the geochemical modeling for each of the four water types.

- Group 1: The average values of SI indicate that the groundwater has lower levels of some individual minerals, except for calcite, which is slightly higher than the optimal saturation level.
- Group 2: The saturation index (SI) findings show that groundwater is deficient in many specific minerals, except calcite and dolomite, which are in excess.
- Group 3: The statistical measures of the saturation index (SI) illustrate that the minerals present in groundwater is in a state of undersaturation.

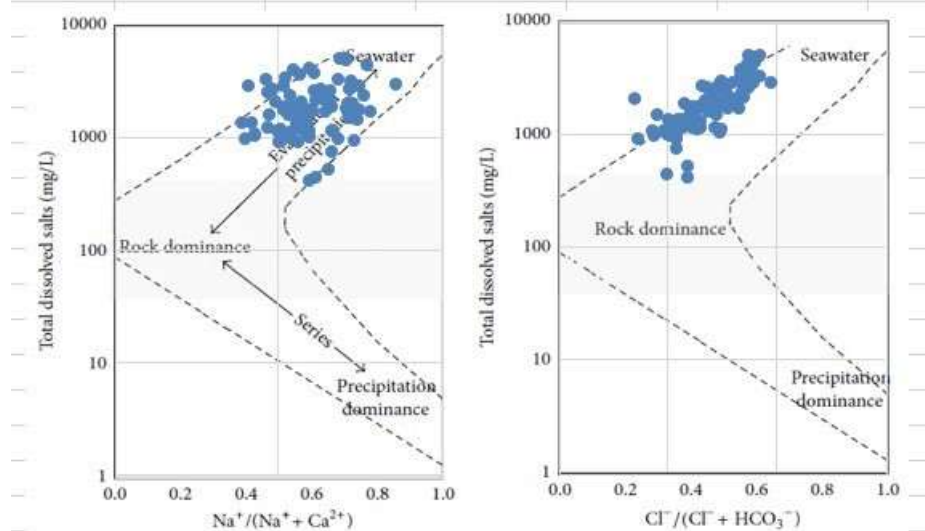
- Group 4: The saturation index (SI) values indicate that groundwater has higher concentrations of aragonite, calcite, and dolomite than their saturation levels, rendering them supersaturated. However, they exhibit lower concentrations of anhydrite and gypsum than they can hold, making them sub-saturated.

Table 5. Saturation Index means value

		Anhydrite	Aragonite	Calcite	Dolomite	Gypsum
Group 1	Min	-1.92	-1.04	-0.9	-1.62	-1.7
	Max	-0.66	0.39	0.54	1.08	-0.44
	Mean	-1.17	-0.03	0.1	-0.01	-0.95
Group 2	Min	-1.32	-0.6	-0.45	-0.61	-1.1
	Max	-0.64	0.63	0.78	1.66	-0.42
	Mean	-1.07	-0.02	0.12	0.5	-0.85
Group 3	Min	-1.61	-0.73	-0.59	-0.85	-1.39
	Max	-0.55	0.49	0.63	1.01	-0.33
	Mean	-1.03	-0.22	-0.07	-0.15	-0.81
Group 4	Min	-1.1	-0.65	-0.51	-1.61	-0.88
	Max	-0.28	0.73	0.87	1.35	-0.06
	Mean	-0.64	0.09	0.23	0.15	-0.42
Means		-3.91	-0.18	0.38	0.49	-3.03

Gibbs Diagram

The Gibbs diagram is employed to evaluate the dominant mechanism governing Water's chemical makeup and the origins of dissolved ions (Singaraja et al. 2017). This is achieved by graphing the Total Dissolved Solids (TDS) against two ratios: the ratio of Sodium ions (Na^+) to the sum of Sodium ions and Calcium ions ($\text{Na}^+ + \text{Ca}^{2+}$), and the ratio of Chloride ions (Cl^-) to the sum of Chloride ions and Bicarbonate ions ($\text{Cl}^- + \text{HCO}_3^-$) (Toumi et al. 2015). The Gibbs diagram displays three distinct areas: the precipitation dominance area, the area dominated by rock-water interaction, and the area dominated by evaporation (Gibbs 1970). Based on the Gibbs plot analysis (Fig. 10), the water samples are situated in a region dominated by evaporation. The extremely arid climate is the primary factor affecting the groundwater composition in the study area. The evaporation process increases water salinity, which is further influenced by rocks and groundwater interaction.

**Fig. 10.** Gibbs plot for groundwater samples

Chadha plot

The Chadha diagram is employed for the analysis of hydrochemical mechanisms that govern the mineralization of groundwater (Abdel Wahed et al. 2015). The graph illustrates the disparity in the milliequivalent ratio between alkaline earth metals and alkali metals as well as the contrast in the milliequivalent ratio between weakly acidic anions and strongly acidic anions, using two axes (Nolakana et al. 2016). Chadha (1999) expands the milliequivalent percent difference for the X and Y coordinates to subareas with clearly defined geochemical processes and water types.

All samples examined in this study (Figure 11) are located in an area where the concentration of alkali metals, specifically potassium and sodium cations, is higher than that of alkaline earth, primarily calcium and magnesium cations. The main geochemical processes in this area are base ion exchange and the presence of brine. The Na-K- HCO_3 facies develop during base ion exchange, where sodium and potassium from the water replace calcium and magnesium in the surrounding rock, such as limestone, dolomite, or silicate. These facies result from the invasion

of an area previously inhabited by saltwater or sodium brine, which is generated from saltwater by fresh groundwater high in CaMgHCO_3 (Sidibé et al., 2019). The Na-K-Cl-SO₄ facies suggest a long period of water presence and aged water formed by the dissolution of metals, primarily from halite, gypsum, and anhydrite.

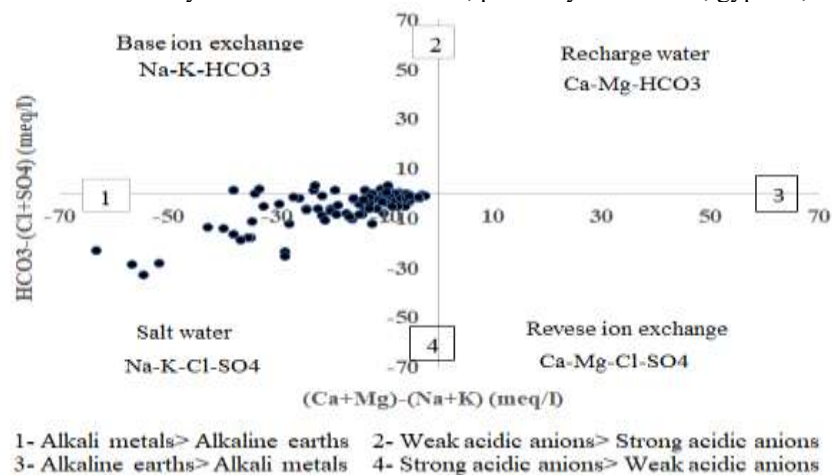


Fig.11. Chadha plot for groundwater samples.

Ionic relationship

The link between sodium (Na^+) and chlorine (Cl^-)

Figure 12's Na vs. Cl plot can help determine the origin of chloride and sodium ions in water. A Na/Cl ratio near 1, found in 64.75% of samples, indicates that the main origin of these ions is halite dissolution (Zaidi et al., 2015; Iqbal et al., 2018). The sodium surplus compared to chlorine in the sample points falls along the 1:1 equiline, accounting for 31.76%. This can be ascribed to base ion exchange and silicate weathering (Sajil Kumar et al. 2014). The Chadha plot and chloralkaline index provide evidence to support this claim. Samples with chlorine levels exceeding sodium levels account for 3.52%. They are likely due to human-made pollution and may be caused by the interaction of aquifer water with the shallow subsurface aquifer water (Rao et al. 2014).

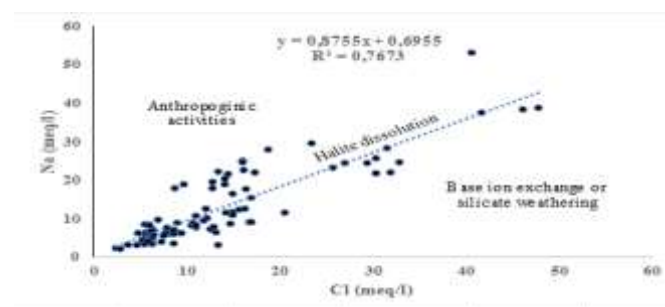


Fig.12. The plot of Na^+ vs Cl^- .

The link between calcium (Ca^{2+}) and sulfate (SO_4^{2-})

The Ca/SO₄ plot is used to identify the origin of sulfate and calcium in groundwater (Bouderbala, 2020). These ions come from the breakdown of gypsum when the samples fall on the 1:1 line (Kuldip et al., 2011). Calcium to sulphate ratio averages 0.69 meq/l. According to Chadha plot, the surplus of sulfate ions compared to calcium ions in Figure 13 is attributed to the calcium exchange process.

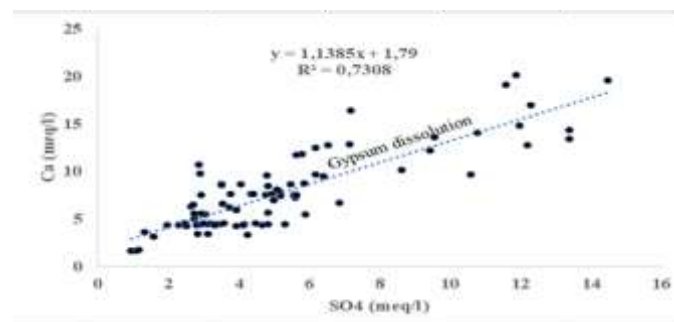


Fig.13. Ca^{2+} vs SO_4^{2-} plot.

The $\text{Ca}^{2+} + \text{Mg}^{2+}$ versus HCO_3^- plot

The $\text{Ca}^{2+} + \text{Mg}^{2+}$ and HCO_3^- plots reveal the origin of calcium, magnesium, and carbonate ions in groundwater and the precipitation or dissolution of carbonate rock minerals (Islam et al., 2018). The saturation index data indicates that the mean values for aragonite are negative, while the mean values for dolomite and calcite are positive. The

plot and the groundwater saturation index show the presence of aragonite dissolution and calcite and dolomite precipitation processes.

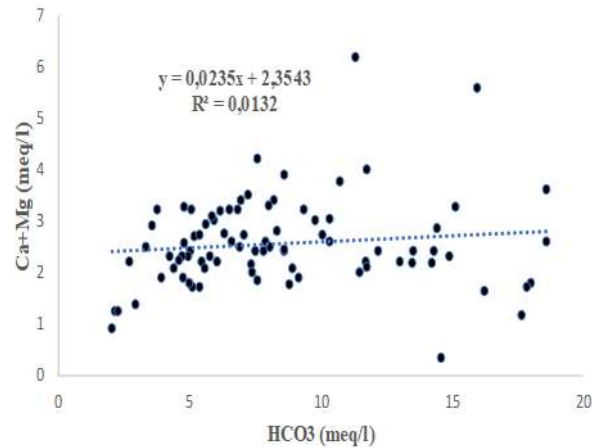
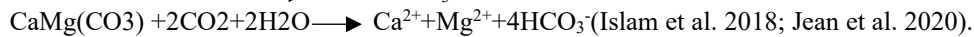
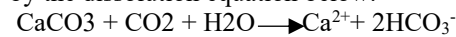


Fig. 14. The plot of $\text{Ca}^{2+} + \text{Mg}^{2+}$ vs HCO_3^- .

The plot of $\text{Ca}^{2+} + \text{Mg}^{2+}$ versus $\text{HCO}_3^- + \text{SO}_4^{2-}$

The $\text{Ca}^{2+} + \text{Mg}^{2+}$ vs. $\text{HCO}_3^- + \text{SO}_4^{2-}$ graph depicts the relationship between calcium, magnesium, sulfate, and bicarbonate ions in groundwater, this graph also predicts potential hydrochemical reactions that may occur and control the ion concentrations, points along the equiline 1:1 demonstrate the dissolution of minerals containing sulfate, calcium, and magnesium (Kumar et al. 2009). The saturation index and the Ca^{2+} vs SO_4^{2-} plot confirm gypsum dissolution. Calcite and dolomite dissolution can be ascribed to the undersaturation of CO_2 , as indicated by the dissolution equation below:



In figure 14, the points above the equiline demonstrate reverse ion exchange between calcium and magnesium in rock-forming clay and sodium in groundwater. Points below the 1:1 equiline indicate the weathering of silicates and carbonates due to the excess bicarbonate content in groundwater (Rajmohan and Elango, 2004).

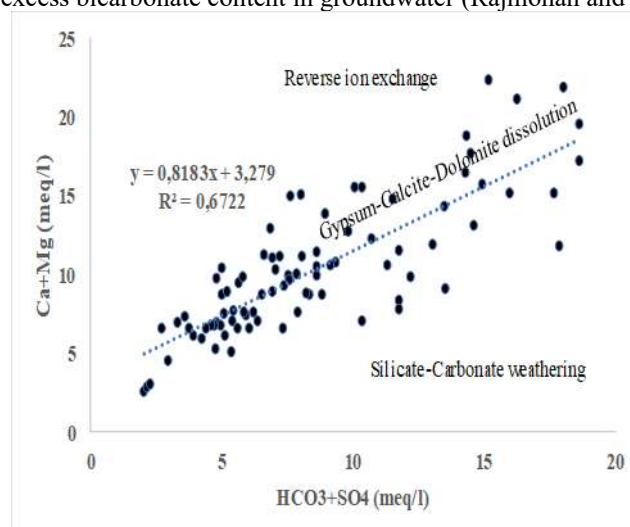


Fig. 15. The plot of $\text{Ca}^{2+} + \text{Mg}^{2+}$ vs $\text{HCO}_3^- + \text{SO}_4^{2-}$.

Evaluation of groundwater quality for consumption

Water Quality Index

The water quality index is a mathematical method used to assess the quality and possible applications of a particular body of water in a clear and comprehensible manner (Jumber et al. 2024). It summarizes extensive information on water quality into a singular metric (Kizar 2018). Water quality estimation methods include: the Oregon Water Quality Index (OWQI), the Canadian Council of Ministers of Water Quality Index Environment (CCMEWQI), the National Sanitation Foundation Water Quality (NSFWQI), and the Weighted Arithmetic Water Quality Index (WAWQI) (Ojukwu et al. 2021).

The study utilized the weighted arithmetic water quality index technique, which categorized water quality based on the most often measured variable to determine its purity level (Brraich et al., 2021).

The water quality index is determined using four steps outlined in Brown et al.'s 1972 formula.

Step 1: Gather data from various physicochemical water quality metrics.

Step 2: Calculate each parameter's unit weight (w_n) factors using the formula $w_n = K/S_n$.

The formula calculates the value of K as the reciprocal of the sum of the reciprocals of S1, S2, S3 and so on up to Sn.

Sn is the standard desirable value of the net parameters obtained by summing all selected parameters unit weight factors.

$W_n=1$ (Unity)

Step 3: Calculate the sub-index (Qn) value using the formula $Q_n = \{(V_n - V_0) / (S_n - V_0)\} * 100$

Vn represents the average concentration of the nth parameter.

The standard desirable value of the nth parameter in this study was based on the WHO guidelines 2011.

The current values of the parameters in pure water are typically $V_0=0$, except for pH. QpH is calculated as a percentage using the formula: $Q_{pH} = ((V_{pH} - 7) / (8.5 - 7)) * 100$

Calculate the Water Quality Index (WQI) using the formula: $WQI = ((\sum W_n * Q_n) / \sum W_n)$ (Chandra et al., 2017)

The table below (Table 5) presents the computed water quality index for the four water classes. Group 2 and Group 4 waters are deemed unfit for consumption, Group 3 waters are considered very bad, and Group 1 waters are classified as poor.

Table 6 Water Quality Index for the four water groups.

Water group	Index value	Water Quality Index	Water Quality
/	/	0 to 25	Excellent water
/	/	26 to 50	Good water
Group 1	68.10	51 to 75	Poor water
Group 3	88.20	76 to 100	Very poor
Group 2 and Group 4	130.36 and 114.61	More than 100	Unsuitable for consumption

Evaluation of groundwater quality for irrigation purpose

Table 4 outlines criteria, calculation, and water classification intervals utilized to evaluate groundwater suitability for irrigation. Table 5 summarizes the data on the irrigation parameters that were assessed.

Electrical conductivity (EC)

Electrical conductivity refers to a material's ability to conduct electricity. Since the majority of salts in water are present in ionic form, electrical conductivity is considered a dependable indicator for assessing water quality. (Balachandar et al. 2010). High salt levels increase the osmotic pressure of the soil solution, leading to a physiological drought condition and plant withering (Zaman et al., 2018). The elevated salt of irrigation water can impact soil structure, permeability, and aeration (Costa and Aparicio 2015).

Based on Richard classification (1954), only 2.35% of Guerrara Complex Terminal water is appropriate for irrigation (C2), while 36.47% is doubtful for irrigation (C3), and 61.17% is deemed unsuitable for irrigation.

Adsorption Sodium Ratio (SAR)

The Sodium Adsorption Ratio (SAR) signifies sodium's risk in irrigation water compared to calcium and magnesium levels. High SAR levels can cause soil permeability issues and degrade soil structure (Zamam et al., 2018).

Richards classification (1954) categorizes the water at the Guerrara Complex Terminal as follows:

- 85.88% is excellent for irrigation (S1, SAR less than 10).
- 12.94% is good for irrigation (S2, SAR from 10 to 18).
- Only 1.17% is moderate for irrigation (S3, SAR exceeding 18).

The Riverside graphic categorizes water by examining the correlation between SAR values and Electrical Conductivity (Figure 15). In our investigation, samples fall into six distinct classes. 2.35% of the samples belong to class S1-C2, 35.29% to class S1-C3, and 47.05% to class S1-C4. In addition, 2.35% of the water samples fall under S2-C3, 11.76% under S2-C4, and 1.17% under S3-C4.

Table 7 Irrigation water parameters utilized in the study for assessing water quality.

Water parameter	Formula	Reference	Range	Water classification
Electrical conductivity	-	Richard 1954	< 250 250-750 750-2250 >2250	Excellent (C1) Good (C2) Doubtful (C3) Unsuitable (C4)
Sodium Adsorption Ratio (SAR)	$\frac{Na^+}{\sqrt{\frac{Ca^{2+} + Mg^{2+}}{2}}}$	Richard 1954	<10 10-18 18-26 >26	Excellent (S1) Good (S2) Moderate (S3) Unsuitable (S4)

Soluble Sodium Percentage (SSP)	$\frac{Na^+}{Ca^{2+} + Mg^{2+} + Na^+ + K^+} * 100$	Wilcox 1955	20-40 40-60 60-80 >80	Good Permissible Doubtful Unsuitable
Residual Sodium Bicarbonate (RSBC)	$HCO_3^- - Ca^{2+}$	Gupta and Gupta 1987	<5 5-10 >10	Satisfactory Marginal Unsatisfactory
Magnesium Hazard (Mg%)	$\frac{Mg^{2+}}{Ca^{2+} + Mg^{2+}} * 100$	Szablocs and Darab 1964	<50 >50	Suitable for irrigation Unsuitable for irrigation
Kelly's Ratio (KR)	$\frac{Na^+}{Ca^{2+} + Mg^{2+}}$	Kelly 1963	>1 1-2 <2	Good Doubtful Unsuitable
Permeability Index (PI)	$\frac{Na^+ + \sqrt{HCO_3^-}}{Ca^{2+} + Mg^{2+} + Na^+} * 100$	Doneen 1964	>75 75-25 <25	Suitable Good Unsuitable
Potential Salinity (PS)	$Cl^- + \frac{1}{2}SO_4^{2-}$	Doneen 1964	<5 5-10 >10	Excellent to good Good to injurious Injurious to Unsuitable
Chloro-alkaline 1 (CA1)	$\frac{Cl^- - (Na^+ + K^+)}{Cl^-}$	Scholler 1967	>1 <1	CA equilibrium CA disequilibrium
Chloro-alkaline 2 (CA2)	$\frac{Cl^- - (Na^+ + K^+)}{SO_4^{2-} + CO_3^- + HCO_3^- + NO_3^-}$	Scholler 1967	>1 <1	CA equilibrium CA disequilibrium

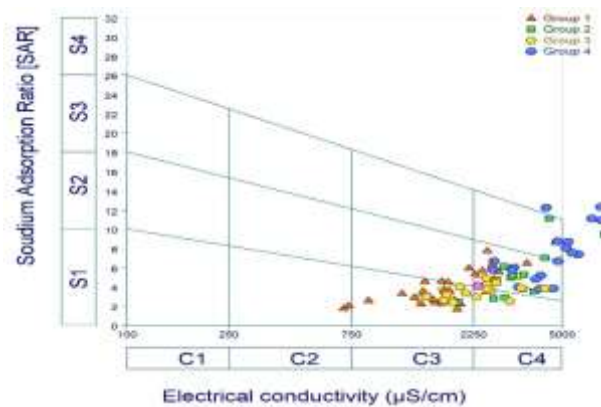


Fig.15 Riverside diagram of the groundwater samples.

Soluble Sodium Percentage (SSP)

Soluble Sodium Percentage (SSP) is a crucial parameter that signifies the percentage of sodium cations in water, and it is used to classify water quality for irrigation purposes (De Andrad Costa et al. 2020). Excessive salt levels in irrigation water can influence the soil structure by accumulating in pore spaces, decreasing soil permeability, and ultimately lowering crop yields. High sodium levels in the soil can result in the displacement of calcium and magnesium by sodium in the clay, causing the degradation of the soil's physical characteristics (Joshi et al., 2009; Hem, 1991; Musika et al., 2021).

Based on Wilcox's classification (Figure 16), specimens being examined can be categorized into four types: 1.17% of water samples classified as good for irrigation, 47.05% as suitable, 50.58% as doubtful, and 1.17% as unsuitable for irrigation.

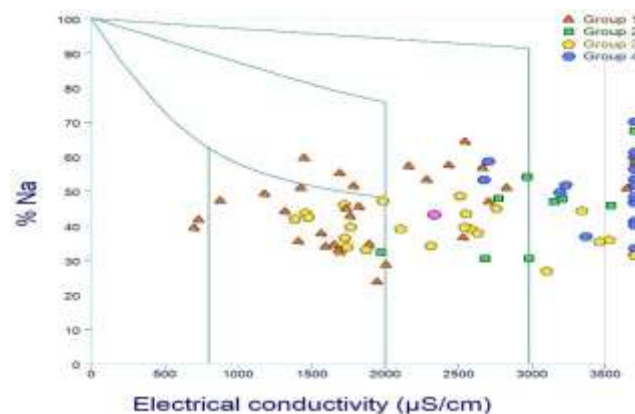


Fig.16 Wilcox diagram of the groundwater samples.

Residual Sodium Bicarbonate (RSBC)

If the quantity of sodium bicarbonate in water exceeds the amount of calcium, residual sodium bicarbonate (RSBC) forms, elevating the water's pH. High RSBC irrigation water causes sodium bicarbonate to accumulate in the soil, increasing salinity (Eaton 1950; Nasseem et al. 2010).

Based on Gupta and Gupta's classification (1987), the Residual Sodium Bicarbonate Concentration (RSBC) of all the water examined is below 5, indicating satisfactory levels, and no risk of sodium carbonate precipitation in the soil.

Magnesium Hazard (Mg%)

Magnesium hazard is critical in assessing the influence of magnesium concentration in water on soil parameters (Tamsasebi et al., 2018). Furthermore, soil alkalinity can result from elevated levels of magnesium in irrigation water (Ramesh and Elango 2018). Moreover, the significant water absorption by clay and magnesium impacts soil infiltration capability, while elevated magnesium levels in irrigation water might also harm crops (Kawo and Karuppanan 2018).

Based on the Szablocs and Darab classification from 1964, 64.70% of the water analyzed has a magnesium concentration below 50% and is considered suitable for irrigation, whereas 23.52% of the water examined has a magnesium content exceeding 50% and is deemed unfit for irrigation.

Kelley's Ratio (KR)

The Kelly ratio quantified the sodium level in water relative to calcium and magnesium (Nasseem et al., 2010). Kelley (1963) reported that 15.29% of the water has a Kelly's Ratio (KR) of less than 1, which is suitable for irrigation. 56.47% have a KR between 1 and 2, considered doubtful for irrigation, while 28.23% have a KR greater than 2, deemed unsuitable for irrigation.

Permeability Index (PI)

High salinity in irrigation water impacts soil permeability. Prolonged exposure to irrigation water with elevated amounts of bicarbonate, sodium, magnesium, and calcium can lead to various soil permeability issues (Rawat et al., 2018).

Donnen (1964) categorized irrigation water into three classes based on their PI. In our study, 49.41% of water samples had a PI between 25 and 75, deemed good, whereas 50.58% had a PI more than 75, which was judged unsuitable.

Potential Salinity (PS)

Potential Salinity (PS) is a water quality indicator utilized to evaluate the appropriateness of irrigation (Rawat et al., 2018). The value is determined by adding the chloride concentration to half the sulfate concentration (Ogunfowokan et al. 2013). The suitability of irrigation water is not determined only by the amount of dissolved salts present, insoluble salts precipitate and build up in the soil after each round of irrigation. Conversely, excessive amounts of soluble salts lead to a rise in soil salinity (Doneen 1964).

Our research found that 4.70% of the water is suitable for irrigation purposes, 30.58% is marginally appropriate, and 64.70% is unsuitable for irrigation.

Chloro-alkaline Indices (CAI)

It is essential to predict future alterations in the chemical makeup of groundwater flows (Sastri 1994). Chloro-alkaline indices analyze the ion exchange between groundwater and rocks in rock-water interactions (Kumar et al. 2020). The chloro-alkaline equilibrium occurs when positive chloro-alkaline values signify base exchange reactions involving the exchange of sodium and potassium from water with magnesium and calcium in rock. Conversely, the chloro-alkaline disequilibrium occurs when the chloro-alkaline values are negative, suggesting that cation-anion exchange processes promote the exchange of calcium and magnesium from water with potassium and sodium in rock (Gupta et al., 2009).

Only two groundwater samples in the study exhibit negative Chloro-alkaline values. In contrast, all other samples show positive values, suggesting base exchange processes between sodium and potassium in water and magnesium and calcium in rock (chloro-alkaline equilibrium). The process of base exchange leads to soil molecules deflocculating and decreases soil permeability (Todd 2004).

Table 8 Data of irrigation parameters studied

	EC	SAR	KR	RSBC	MAR	SSP	PI	PS	CAI 1	CAI 2
Min	701	2.34	0.58	-12.87	2.17	36.34	50.95	2.9	-1.58	3.47
Max	7298	18.67	4.66	1.33	70.29	82.1	95.06	59.86	52.3	69.44
Mean	2903.16	6.78	1.69	-2.61	39.12	59.7	74.74	17.05	11.95	22.18

Conclusion

This research analyzed the water quality of a Complex Terminal aquifer in Guerrara utilizing Statistical Analysis to evaluate hydrochemical quality. Geographic Information System (GIS) techniques were utilized to display

parameter distribution across the area. Ionic plots were used to assess hydrochemical processes, while the water quality index determined water drinkability. Irrigation Water Parameters were examined for irrigation suitability. The average pH of groundwater is 7.40, indicating it is slightly alkaline/heavily mineralized, with an average electrical conductivity of 2903.1 $\mu\text{S}/\text{cm}$ and 1993 mg/L for total dissolved solids. Anions are most prevalent in the following order: $\text{SO}_4^{2-} > \text{Cl}^- > \text{HCO}_3^- > \text{NO}_3^-$, whereas cations are most prevalent in the sequence: $\text{Na}^+ > \text{Ca}^{2+} > \text{Mg}^{2+} > \text{K}^+$. The spatial distribution of the studied parameters discloses a significant positive correlation between dominant ions and Electrical Conductivity, suggesting that these ions are the main contributors to water mineralization. The central and eastern regions of the study area display the highest levels of mineralization. Water wells were categorized into four groups using Hierarchical Component Analysis (HCA), each group exhibiting a distinct hydrochemical facies: $\text{SO}_4\text{-Na-Ca}$, $\text{SO}_4\text{-Na-Cl}$, SO_4 without a dominating cation, and $\text{SO}_4\text{-Cl-Na-Ca}$. Pearson correlations revealed considerable relationships among the tested parameters. Electrical conductivity is observed with Ca^{2+} , Na^+ , Cl^- , and SO_4^{2-} ions, specifically the interaction between Na^+ and SO_4^{2-} and Cl^- and between Ca^{2+} and SO_4^{2-} . Principal Component Analysis identified three main components explaining 75.67% of the variance in water parameters. The first component, accounting for 48.02% of the variance, is associated with Electrical Conductivity, Sodium, Chloride, Sulfate, and Calcium ions, suggesting mineralization from evaporitic rocks like halite, gypsum, and anhydrite. The second component, explaining 16.42% of the variance, is linked to bicarbonate and magnesium, indicating leaching from carbonate rocks. The third component, representing 11.02% of the variance, is correlated with nitrates, potassium, and water temperature, pointing to anthropogenic contamination. The Saturation Index, calculated using PHREEQC software, indicates that studied groundwater samples are undersaturated with gypsum, anhydrite, and aragonite, and oversaturated with calcite and dolomite. These findings elucidate the ionic composition of the water and forecast potential future mineral content. The Gibbs diagram shows that evaporation and rock domination are the main factors increasing water salinity. The Chadha plot demonstrated that alkali metals surpass alkaline earth metals and that base ion exchange and saltwater are the main geochemical processes occurring in water. The water samples studied are classified as poor, very poor, or unsuitable for irrigation based on the Water Quality Index. Based on Electrical Conductivity values, most of the water samples analyzed contain high salt levels, rendering them questionable or unsuitable for irrigation. Although SAR values are typically below safe limits, the sodium hazard potential indicates that caution should be exercised when using this water for irrigation. RSBC states that sodium carbonate precipitation is not possible in the soil. Analysis of magnesium risks shows that it is absent in two-thirds of the water samples and present in one-third of the samples. Approximately 70% of the water samples are dubious or suitable for irrigation based on the KR parameter, which assesses the sodium level in water relative to calcium and magnesium, whereas 30% are deemed unsuitable for irrigation. Using the PI parameter to assess the impact of sodium, magnesium, calcium, and bicarbonate on soil permeability, around half of the water samples exhibit acceptable quality. In contrast, the other half shows poor quality. Salinity in water is primarily attributed to low soluble salts, with two-thirds resulting from combining half of the sulfate concentration with the chloride content. Positive Chloro-alkaline readings indicate that the base ion exchange mechanism is the primary process influencing upcoming chemical reactions.

Statements and Declarations

We declare that there has been no significant financial support for this work that could have influenced its outcome. We know of no conflicts of interest associated with this publication.

Competing Interests

The authors declare that they have no known competing financial interests or personal relationships that could have appeared to influence the work reported in this paper.

References

1. Abdel Wahed, M. S., Mohamed, E. A., El-Sayed, M. I., M'nif, A., & Sillanpää, M. (2015). Hydrogeochemical processes controlling the water chemistry of a closed saline lake located in Sahara Desert: Lake Qarun, Egypt. *Aquatic geochemistry*, 21, 31-57.
2. Balachandar, D., Sundararaj, P., Murthy, K. R., & Kumaraswamy, K. (2010). An investigation of groundwater quality and its suitability to irrigated agriculture in Coimbatore District, Tamil Nadu, India—A GIS approach. *International Journal of environmental sciences*, 1(2), 176-190.
3. Barkat, A., Bouaicha, F., Bouteraa, O., Mester, T., Ata, B., Balla, D., ... & Szabó, G. (2021). Assessment of Complex Terminal groundwater aquifer for different use of Oued Souf Valley (Algeria) using multivariate statistical methods, geostatistical modeling, and water quality index. *Water*, 13(11), 1609.
4. Benaraba, N., Touati, F., Benyahia, S., & Yebdri, D. (2022). Jointly estimating recharge and groundwater withdrawals of the NWSAS by inverting GRACE/GRACE-FO gravity data. *Hydrological Sciences Journal*, 67(15), 2215-2231.
5. Bouderbala, A. (2020). Groundwater quality assessment of the coastal alluvial aquifer of Wadi Hachem, Tipaza, Algeria. *Environmental & Socio-economic Studies*, 8(4), 11-23.
6. Bouselsal, B., & Saibi, H. (2022). Evaluation of groundwater quality and hydrochemical characteristics in the shallow aquifer of El-Oued region (Algerian Sahara). *Groundwater for Sustainable Development*, 17, 100747.

7. Brauch, H. G., Spring, Ú. O., Mesjasz, C., Grin, J., Kameri-Mbote, P., Chourou, B., ... & Birkmann, J. (Eds.). (2011). *Coping with global environmental change, disasters and security: threats, challenges, vulnerabilities and risks* (Vol. 5). Springer Science & Business Media.
8. Brraich, O. S., Kaur, N., & Akhter, S. (2021). Assessment of limnological parameters and water quality indices of Harike wetland (Ramsar Site) Punjab, India. *Applied Ecol. Environ. Sci*, 9(6), 591-598.
9. Castany G (1982a) Bassin sédimentaire du Sahara septentrional (Algérie- Tunisie). *Aquifère du continental intercalaire et du Complexe Terminal. Bull BRGM, deuxième série, section III N°2* : 127-147
10. Chadha, D. K. (1999). A proposed new diagram for geochemical classification of natural waters and interpretation of chemical data. *Hydrogeology journal*, 7, 431-439.
11. Chandra, D. S., Asadi, S. S., & Raju, M. V. S. (2017). Estimation of water quality index by weighted arithmetic water quality index method: a model study. *International Journal of Civil Engineering and Technology*, 8(4), 1215-1222.
12. Chellat, S., Djerra, A., Bourefis, A., & Belhadj, H. A. (2014). LES GRÈS MIO-PLIOCÈNES DE LA REGION DE GUERRARA-GHARDAIA: ANALYSE SEDIMENTOLOGIQUE, SEQUENTIELLE ET PALEOENVIRONNEMENTALE. *Bulletin du Service Géologique de l'Algérie*, 25(2), 105-125.
13. Costa, J. L., & Aparicio, V. C. (2015). Quality assessment of irrigation water under a combination of rain and irrigation. *Agricultural Water Management*, 159, 299-306.
14. De Andrade Costa, D., Soares de Azevedo, J. P., Dos Santos, M. A., & dos Santos Facchetti Vinhaes Assumpção, R. (2020). Water quality assessment based on multivariate statistics and water quality index of a strategic river in the Brazilian Atlantic Forest. *Scientific reports*, 10(1), 22038.
15. Dehbozorgi, N., & Kunuku, M. T. (2023). Exploring the Influence of Emotional States in Peer Interactions on Students' Academic Performance. *IEEE Transactions on Education*.
16. Dhaoui, Z., Zouari, K., Taupin, J. D., & Farouni, R. (2016). Hydrochemical and isotopic investigations as indicators of recharge processes of the Continental Intercalaire aquifer (eastern piedmont of Dahar, southern Tunisia). *Environmental Earth Sciences*, 75, 1-14.
17. Djili, B., & Hamdi-Aïssa, B. (2018). Characteristics and mineralogy of desert alluvial soils: Wadi Zegrir, Northern Sahara of Algeria. *Arid Land Research and Management*, 32(1), 1-19.
18. Doneen, L. D. (1964). *Notes on water quality in agriculture*. Department of Water Science and Engineering, University of California, Davis.
19. Eaton, F. M. (1950). Significance of carbonates in irrigation waters. *Soil science*, 69(2), 123-134.
20. El-Rawy, M., Fathi, H., Abdalla, F., Alshehri, F., & Eldeeb, H. (2023). An Integrated Principal Component and Hierarchical Cluster Analysis Approach for Groundwater Quality Assessment in Jazan, Saudi Arabia. *Water*, 15(8), 1466.
21. Gibbs, R. J. (1970). Mechanisms controlling world water chemistry. *Science*, 170(3962), 1088-1090.
22. Guendouz, A., & Moulla, A. S. (2010, December). The Shared Resources in the North-Western Sahara Aquifer System (Algeria-Tunisia-Libya): The use of Environmental Isotopes (Algeria part). In *Proceeding of the International Conference "Transboundary Aquifers: Challenges and New Directions" (ISARM2010)*, 1-4. Paris, 6-8 December 2010.
23. Guendouz, A., Moulla, A. S., Edmunds, W. M., Zouari, K., Shand, P., & Mamou, A. (2003). Hydrogeochemical and isotopic evolution of water in the Complexe Terminal aquifer in the Algerian Sahara. *Hydrogeology journal*, 11(4), 483-495.
24. Gupta, S. K., & Gupta, I. C. (1987). *Management of saline soils and waters*. Oxford & IBH Publishing Co..
25. Gupta, S., Dandele, P. S., Verma, M. B., & Maithani, P. B. (2009). Geochemical assessment of groundwater around Macherla-Karempudi area, Guntur district, Andhra Pradesh. *J Geol Soc India*, 73(2), 202-212.
26. Hadj-Said, S., Zeddouri, A., Djabri, L., & Hamdi-Aïssa, B. (2013). Determination of the aquifers geometry in arid zones by using geoelectrical method. *Arabian Journal of Geosciences*, 6(4), 1081-1089.
27. Hem, J. D. (1991). edition 3. *Study and interpretation of the chemical characteristics of natural water*. Jodhpur.
28. Hwang, J. Y., Park, S., Kim, H. K., Kim, M. S., Jo, H. J., Kim, J. I., ... & Kim, T. S. (2017). Hydrochemistry for the assessment of groundwater quality in Korea. *Journal of Agricultural Chemistry and Environment*, 6(01), 1.
29. Iqbal, J., Nazzal, Y., Howari, F., Xavier, C., & Yousef, A. (2018). Hydrochemical processes determining the groundwater quality for irrigation use in an arid environment: the case of Liwa Aquifer, Abu Dhabi, United Arab Emirates. *Groundwater for Sustainable Development*, 7, 212-219.
30. Islam, A. T., Shen, S., Haque, M. A., Bodrud-Doza, M., Maw, K. W., & Habib, M. A. (2018). Assessing groundwater quality and its sustainability in Joypurhat district of Bangladesh using GIS and multivariate statistical approaches. *Environment, development and sustainability*, 20, 1935-1959.
31. Joshi, D. M., Kumar, A., & Agrawal, N. (2009). Assessment of the irrigation water quality of river Ganga in Haridwar district. *Rasayan J Chem*, 2(2), 285-292.
32. Karamizadeh, S., Abdullah, S. M., Manaf, A. A., Zamani, M., & Hooman, A. (2013). An overview of principal component analysis. *Journal of Signal and Information Processing*, 4(3B), 173.
33. Kawo, N. S., & Karuppanan, S. (2018). Groundwater quality assessment using water quality index and GIS technique in Modjo River Basin, central Ethiopia. *Journal of African Earth Sciences*, 147, 300-311.
34. Kelley, W. P. (1963). Use of saline irrigation water. *Soil science*, 95(6), 385-391.
35. Khan, A. F., Srinivasamoorthy, K., & Rabina, C. (2020). Hydrochemical characteristics and quality assessment of groundwater along the coastal tracts of Tamil Nadu and Puducherry, India. *Applied water science*, 10, 1-21.

36. Kharroubi, M., Bouselsal, B., Ouarekh, M., Benaabidate, L., &Khadri, R. (2022). Water quality assessment and hydrogeochemical characterization of the OuarglaComplex Terminal aquifer (Algerian Sahara). *Arabian Journal of Geosciences*, 15(3), 251.
37. Khemgani, M. A., Aissa, B. H., &Alomran, A. (2019). Hydrochemical and Piezometric Study of The Alluvial Aquifer of The Guerrara Region, Algeria. *International Journal of Environmental Pollution and Environmental Modelling*, 2(4), 227-236.
38. Kizar, F. M. (2018, November). A comparison between weighted arithmetic and Canadian methods for a drinking water quality index at selected locations in shatt al-kufa. In *IOP Conference Series: Materials Science and Engineering* (Vol. 433, No. 1, p. 012026). IOP Publishing.
39. Kuldip S., Hundal, H. S., Dhanwinder S. (2011). Geochemistry and assessment of hydrogeochemical processes in groundwater in the southern part of Bathinda district of Punjab, northwest India. *Environmental earth sciences*, 64, 1823-1833.
40. Kumar, M., Kumari, K., Singh, U. K., & Ramanathan, A. L. (2009). Hydrogeochemical processes in the groundwater environment of Muktsar, Punjab: conventional graphical and multivariate statistical approach. *Environmental Geology*, 57, 873-884.
41. Kumar, P., Mahajan, A. K., & Kumar, A. (2020). Groundwater geochemical facie: implications of rock-water interaction at the Chamba city (HP), northwest Himalaya, India. *Environmental Science and Pollution Research*, 27, 9012-9026.
42. Kurita, T. (2019). Principal component analysis (PCA). *Computer Vision: A Reference Guide*, 1-4.
43. Li, S., Li, C., Yao, D., Wang, X., & Gao, Y. (2024). Bowl effect of irreversible primary salinization driven by geology in Hetao irrigation area, China. *Science of The Total Environment*, 170834.
44. Liu, T., Gao, X., Zhang, X., & Li, C. (2020). Distribution and assessment of hydrogeochemical processes of F-rich groundwater using PCA model: a case study in the Yuncheng Basin, China. *Acta Geochimica*, 39, 216-225.
45. Majeed, S. N., & Mohan Viswanathan, P. (2021, February). Hydrochemistry and Water Quality Assessment in Labuan Island, Malaysia. In *Proceedings of the Earth and Environmental Sciences International Webinar Conference* (pp. 35-61). Cham: Springer International Publishing.
46. Melouah, O., &Zeddouri, A. (2016). Use of geophysical methods for the demonstration of Karstic phenomena in southern Algeria: Guerrara area (district of Ghardaïa. Algeria). *Journal of Fundamental and Applied Sciences*, 8(3), 1097-1114.
47. Melouah, O., Zerrouki, H., & Steinmetz, R. L. L. (2020). Characterization of processes and mechanisms controlling ground water salinization in the Algerian Sahara. *Arabian Journal of Geosciences*, 13(18), 1-31.
48. Modibo Sidibé, A., Lin, X., & Koné, S. (2019). Assessing groundwater mineralization process, quality, and isotopic recharge origin in the Sahel Region in Africa. *Water*, 11(4), 789.
49. Mohammadi, Z. (2009). Assessing hydrochemical evolution of groundwater in limestone terrain via principal component analysis. *Environmental Earth Sciences*, 59, 429-439.
50. Mukiza, P., Bazimenyera, J. D. D., Nkundabose, J. P., Niyonkuru, R., &Bapfakurera, N. E. (2021). Assessment of irrigation water quality parameters of Nyandungu wetlands. *Journal of Geoscience and Environment Protection*, 9(10), 151-160.
51. Nadhira, S., & Omar, S. (2019). Hydrogeochemical characterization of the Complexe Terminal aquifer system in hyper-arid zones: the case of wadi Mya Basin, Algeria. *Arabian Journal of Geosciences*, 12(24), 1-18.
52. Naseem, S., Hamza, S., & Bashir, E. (2010). Groundwater geochemistry of Winder agricultural farms, Balochistan, Pakistan and assessment for irrigation water quality. *European water*, 31, 21-32.
53. National Meteorological Office (NMO) 2023.
54. Nolakana, P. (2016). Geochemical assessment of groundwater quality and suitability for drinking and irrigation purposes in Newcastle, Kwazulu-Natal, South Africa.
55. Ogunfowokan, A. O., Obisanya, J. F., &Ogunkoya, O. O. (2013). Salinity and sodium hazards of three streams of different agricultural land use systems in Ile-Ife, Nigeria. *Applied Water Science*, 3, 19-28.
56. Ojukwu, C. K., Okeah, G. O. C., &Mmom, P. C. (2021). A Comparative Analysis of the Weighted Arithmetic and Canadian Council of Ministers of the Environment Water Quality Indices for Water Sources in Ohaozara, Ebonyi State, Nigeria. *International Journal of Engineering Research&Technology (IJERT)*, 10.
57. OSS Observatoire du Sahara et du Sahel (2003) *Système Aquifère du Sahara Septentrional Hydrogéologie, projet SASS, Volume II, 2ème édition*
58. Ould Baba Sy M (2005) *Recharge et Paléo-recharge du Système Aquifère du Sahara Septentrional. Thèse de doctorat. Université Tunis El Manar*
59. Parkhurst, D. L., &Appelo, C. A. J. (2013). Description of input and examples for PHREEQC version 3—a computer program for speciation, batch-reaction, one-dimensional transport, and inverse geochemical calculations. *US geological survey techniques and methods*, 6(A43), 497.
60. Plummer, L. N., Parkhurst, D. L., &Thorstenson, D. C. (1983). Development of reaction models for ground-water systems. *Geochimica et cosmochimica Acta*, 47(4), 665-685.
61. Rajmohan, N., Masoud, M. H., &Niyazi, B. A. (2021). Impact of evaporation on groundwater salinity in the arid coastal aquifer, Western Saudi Arabia. *Catena*, 196, 104864.
62. Ramesh, K., &Elango, L. (2012). Groundwater quality and its suitability for domestic and agricultural use in Tondiar river basin, Tamil Nadu, India. *Environmental monitoring and assessment*, 184, 3887-3899.

63. Rao, N. S., Rao, P. S., Reddy, G. V., Nagamani, M., Vidyasagar, G., & Satyanarayana, N. L. V. V. (2012). Chemical characteristics of groundwater and assessment of groundwater quality in Varaha River Basin, Visakhapatnam District, Andhra Pradesh, India. *Environmental monitoring and assessment*, 184(8), 5189-5214.
64. Rawat, K. S., Singh, S. K., & Gautam, S. K. (2018). Assessment of groundwater quality for irrigation use: a peninsular case study. *Applied Water Science*, 8, 1-24.
65. Reghais, A., Drouiche, A., Zahi, F., & Debieche, T. H. (2023). Hydrogeochemical evaluation of the Terminal Complex aquifer system in an arid area: a case study from the Biskra region, north-east Algeria. *Environmental Earth Sciences*, 82(7), 182.
66. Rodier J (1996) *L'analyse de l'eau. Eaux naturelles, eaux résiduelles et eau de mer* (8ème édition Dunod)
67. Roy, P. D., Selvam, S., Venkatraman, S., Logesh, N., Lakshumanan, C., & Sánchez-Zavala, J. L. (2021). Identification of sources and groundwater recharge zones from hydrochemistry and stable isotopes of an agriculture-based paleo-lacustrine basin of drought-prone northeast Mexico. *Geochemistry*, 81(2), 125742.
68. S.C.G. (Service de la Carte Géologique) (1952) *Carte géologique d'Algérie, feuille de Constantine Sud au 1/500 000*. S.C.G., Alger
69. Sajil Kumar, P. J., Delson, P. D., & James, E. J. (2014). Evaluation of groundwater chemistry in Vaniyambadi industrial area with special reference on irrigation utility. *National Academy Science Letters*, 37, 493-502.
70. Sangaré, L. O., Sun, H., Ba, S., Konté, M. S., Samaké, M., & Zheng, T. (2023). A multivariate approach to assessing the water quality of the Bamako reach of the Niger River in Mali as irrigation water. *Water Environment Research*, 95(10), e10933.
71. Sastri, J. C. V. (1994). Groundwater chemical quality in river basins, hydrogeochemical modeling. Lecture notes- Refresher course, School of Earth Sciences, Bharathidasan Univ., Tiruchirapalli, Tamil Nadu, India.
72. Singh, K. K., Tewari, G., & Kumar, S. (2020). Evaluation of groundwater quality for suitability of irrigation purposes: a case study in the Udham Singh Nagar, Uttarakhand. *Journal of Chemistry*, 2020.
73. Slimani, R., Guendouz, A., Trolard, F., Moulla, A. S., Hamdi-Aïssa, B., & Bourrié, G. (2017). Identification of dominant hydrogeochemical processes for groundwaters in the Algerian Sahara supported by inverse modeling of chemical and isotopic data. *Hydrology and Earth System Sciences*, 21(3), 1669-1691.
74. Slimani, R., Charikh, M., Aljaradin, M (2023). Assessment of groundwater vulnerability to pollution in an Arid environment. *Archives of Environmental Protection*. Vol. 49 no. 2 pp. 50–58. ISSN 2083-4772. DOI 10.24425/aep.2023.145896
75. Singaraja, C., Chidambaram, S., Jacob, N., Ezhilarasan, E., Velmurugan, C., Manikandan, M., & Rajamani, S. (2016). Taxonomy of groundwater quality using multivariate and spatial analyses in the Tuticorin District, Tamil Nadu, India. *Environment, development and sustainability*, 18, 393-429.
76. SONATRACH, Division Exploration et Division Petroleum Engineering et Développement (1995) *Géologie de l'Algérie*
77. Subramani, T., Rajmohan, N., & Elango, L. (2010). Groundwater geochemistry and identification of hydrogeochemical processes in a hard rock region, Southern India. *Environmental monitoring and assessment*, 162, 123-137.
78. Swezey, C. S. (1999). The lifespan of the Complexe Terminal aquifer, Algerian-Tunisian Sahara. *Journal of African Earth Sciences*, 28(3), 751-756.
79. Szabolcs, I. (1964). The influence of irrigation water of high sodium carbonate content on soils. *Agrokémia és talajtan*, 13(sup), 237-246.
80. Tahmasebi, P., Mahmudy-Gharaie, M. H., Ghassemzadeh, F., & Karimi Karouyeh, A. (2018). Assessment of groundwater suitability for irrigation in a gold mine surrounding area, NE Iran. *Environmental earth sciences*, 77, 1-12.
81. Todd, D. K., & Mays, L. W. (2004). *Groundwater hydrology*. John Wiley & Sons.
82. Toumi, N., Hussein, B. H., Rafrafi, S., & El Kassas, N. (2015). Groundwater quality and hydrochemical properties of Al-Ula region, Saudi Arabia. *Environmental Monitoring and Assessment*, 187, 1-16.
83. UNESCO (1972) *Etude des ressources en eau du Sahara septentrional. Rapport sur les résultats du projet conclusions et recommandations*, Algérie-Tunisie
84. U S Geological Survey, 2023. USGS Geospatial Data: Digital Elevation Models (DEMs). : available on-line at <https://earthexplorer.usgs.gov/> (15/03/2023).
85. Wilcox, L. (1955). *Classification and use of irrigation waters* (No. 969). US Department of Agriculture.
86. World Health Organization, & WHO. (2004). *Guidelines for drinking-water quality* (Vol. 1). World Health Organization.
87. Zaidi, F. K., Nazzal, Y., Jafri, M. K., Naeem, M., & Ahmed, I. (2015). Reverse ion exchange as a major process controlling the groundwater chemistry in an arid environment: a case study from northwestern Saudi Arabia. *Environmental Monitoring and Assessment*, 187, 1-18.
88. Zaman, M., Shahid, S. A., & Heng, L. (2018). *Guideline for salinity assessment, mitigation and adaptation using nuclear and related techniques* (p. 164). Springer
89. Zaman, M., Shahid, S. A., Heng, L., Zaman, M., Shahid, S. A., & Heng, L. (2018). *Irrigation water quality. Guideline for salinity assessment, mitigation and adaptation using nuclear and related techniques*, 113-131.